Available online at www.sciencedirect.com
SCIENCE DIRECT®
Polymer 44 (2003) 6773–6780
polymer
www.elsevier.com/locate/polymer

Gas transport properties of crown-ether methacrylic polymers: poly(1,4,7,10-tetraoxacyclododecan-2-yl) methyl methacrylate

P. Tiemblo[a,*], J. Guzmán[a], E. Riande[a], F. García[b], J.M. García[b]

[a]*Instituto de Ciencia y Tecnología de Polímeros, CSIC, Juan de la Cierva 3, Madrid 28006, Spain*
[b]*Universidad de Burgos, Plaza Misael Bañuelos s/n, Burgos 09001, Spain*

Received 25 February 2003; received in revised form 23 July 2003; accepted 4 August 2003

Abstract

Polymer membranes were prepared by radical polymerization of the 1,4,7,10-(tetraoxacyclododecan-2-yl) methyl methacrylate (CR4MA) monomer and a small quantity of a cross-linking agent ethyleneglycoldimethacrylate. High vacuum pressure techniques were used to evaluate oxygen and helium transport through these membranes at temperatures below and above its glass transition temperature, between 0 and 50 °C. The apparent values of both the permeability and diffusion coefficients are unusually low because of the high packing degree of these polymeric membrane materials. The results obtained were also compared with those determined for polymer membranes derived from their open chain counterparts, the polymer derivatives from methacrylate monomers with a number of oxyethylene units in the ester residue variable between 2 and 6, and with a set of other polymers.

Keywords: Crown ether; Gas transport; Methacrylates

1. Introduction

The discovery by Pedersen [1] of crown ethers represents a very important advance for many fields, from both basic and applied points of view. It is now well known that cyclic ethers and related macrocycles can coordinate with metal ions in hydrophobic solvents originating the separation from their associated anions and making their salts soluble in these solvents. These compounds offer great possibilities to be useful as metal ions catalysts, ion-exchange membranes, molecular imprinting compounds, surfactants, chirality inductive reagents, etc. [2].

Polymers including these chemical structures can potentially show many of the applications indicated above and in this sense different researchers have investigated the synthesis, properties and uses of polymers containing crown ethers in their structure, and very often for species separation [3–7]. On the other hand, in the last years, the possibility to use methacrylate polymers as matrix for the introduction of transition metal complexes aimed at achieving facilitated transport of oxygen has been explored [8–11]. Methacrylic polymers with lineal side-chains, either aliphatic [12–16] or oxyethylenic [17], show increasing diffusion coefficients with increasing length of the pendant group, up to about 12 bonds. When the number of bonds exceeds 12, there exists the possibility of crystallization [18,19] both in acrylates and methacrylates, and the increase of the diffusion coefficient on increasing the length of the side-chain levels off [7,8].

The introduction of the pendant groups which enhance stiffness completely changes the structure and thus, the diffusivity properties of the methacrylates. This is seen when studying poly(*t*-butyl methacrylate) [20] or methacrylates with liquid crystal properties [21]. Up to now [14,17] we have systematically studied the gas transport properties of methacrylates with flexible side-chains; in this work we present the results obtained on the transport properties of a meth(acrylic) polymer containing a crown ether in the ester residue: poly(1,4,7,10-tetraoxacyclododecan-2-yl) methyl methacrylate, the structure of which appears in Scheme 1.

* Corresponding author. Tel.: +34-915-622-900; fax: +34-915-644-853.
E-mail address: ptiemblo@ictp.csic.es (P. Tiemblo).

0032-3861/$ - see front matter © 2003 Published by Elsevier Ltd.
doi:10.1016/j.polymer.2003.08.010

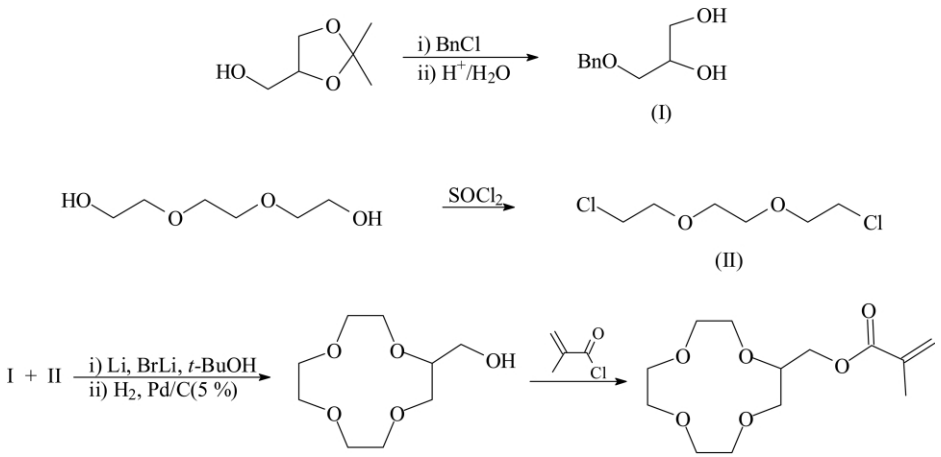

Scheme 1. Synthetic route of (1,4,7,10-tetraoxacyclododecan-2-yl) methacrylate (CR4MA).

2. Experimental

2.1. Materials

All materials and solvents used for the synthesis of the monomers were commercially available, and they were used as received unless otherwise indicated. Tri(ethylene glycol)monomethyl ether (Aldrich, 95%) was purified by vacuum distillation. Dioxane (Aldrich, 99%) was distilled twice: the first time over sodium hydroxide and the second time over sodium. Dichloromethane (Merck, 99.5%) was purified by distillation over $CaCl_2$. Triethylamine (Fluka, 98%) was distilled over sodium hydroxide. 4-hydroxy-2,2,6,6-tetramethyl-1-piperidinyloxyl (TEMPOL) (Aldrich, 98%) was used as received. 2,2′-Azobisisobutyronitrile, AIBN, (Fluka, 98%) was recrystallized from methanol, and dried under high vacuum at room temperature.

2.2. Synthesis of the monomer and of the polymer

The synthetic route followed to prepare the (1,4,7,10-tetraoxacyclododecan-2-yl) methyl methacrylate (CR4MA) is depicted in Scheme 1 and will be described in detail elsewhere. The membrane was prepared by radical polymerization of CR4MA using 1,2-ethanedioldimethacrylate as cross-linking agent and AIBN (1 wt%) as initiator. The nominal cross-linking ratio, i.e. the ratio between the number of moles of monomer to the cross-linking agent, was 100. The addition of a cross-linking agent is necessary in order to obtain membranes with adequate mechanical properties. The reaction was carried out in a silanized glass mould of 100 μm thickness in oxygen free atmosphere at 70 °C for 5 h. The network thus prepared was extracted three times in dioxane for a period of 48 h. Finally, the network was dried at room temperature for one week and the residual solvent was eliminated under high vacuum.

2.3. Density determination

The density of the membranes derived was measured with a 5 ml Weld pycnometer device at 25 °C. Two hundred milligrams of the proper membrane were introduced in the dried pycnometer, and the solvent added to the device. The density was obtained from the different weights of pure solvent and the solvent–membrane system.

This density value, $\rho = 1.208\ \mathrm{g/cm^3}$ was used to estimate the fractional free volume (FFV) at 25 °C by applying

$$\mathrm{FFV} = \frac{V - 1.3V_w}{V} \quad (1)$$

where V is the polymer specific volume, and V_w is the specific Van der Waals volume, which was estimated by using the Hyperchem computer program, version 5.01 [22].

2.4. Thermal analysis

The glass transition temperature of the membranes was determined by differential scanning calorimetry using a Perkin–Elmer DSC-7 calorimeter. The measurements were carried out between −80 and 100 °C under nitrogen atmosphere at a heating rate of 10 °C/min and quenched with a cooling rate of 200 °C/min. Probes were little fragments of film samples put into covered 20 μl aluminium pans. The T_g value obtained, $T_g = 278$ K, was taken from the second runs and correspond to the onset of the DSC curves measured from the extension of the pre- and post-transition baseline. A DSC run is shown in Fig. 1.

2.5. Permeation measurements

A lab made permeator has been used that consists of a gas cell in the middle of which the polymer membrane is placed. This membrane separates the upstream and downstream chambers. For the simplified equations relating the gas flow through the membrane to the transport coefficients to be

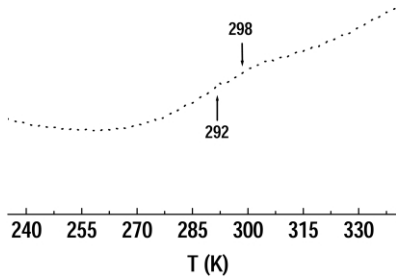

Fig. 1. DSC of PCR4MA.

valid, the downstream pressure has to be kept very low, negligible as compared to the upstream. This is accomplished by thorough evacuation of the downstream, prior to any measurement, by means of a Edwards turbomolecular pump. At the low-pressure side, a MKS Baratron type 627B absolute pressure transducer measures the pressure increase, while at the upstream a Gometrics pressure detector is used to control the gas pressure at which the experiment is performed. The Baratron 627B can be used in the pressure range of $1-10^{-4}$ Torr. The Baratron is connected via a MKS power supply/readout unit to the PC, which records the pressure increase at given time intervals. The whole set-up is temperature controlled in the range of 5–80 °C by means of a water bath.

Before measurements are performed, vacuum is kept overnight in order to remove any rests of solvent from the membrane and to attain a downstream pressure as low as possible. Prior to permeation experiment, a measurement of the pressure increase due to imperfect vacuum isolation of the downstream chamber is recorded. This blank experiment is then subtracted from the permeation experiment performed immediately afterwards in order to calculate the gas transport coefficients from the corrected pressure curves. In that way the pressure increase is related solely to the gas diffusing across the membrane.

The permeability and diffusivity coefficients have been calculated from the curves measuring the pressure increase at the downstream. Eq. (2), derived from the integration of Fick's laws relates the amount of diffusant per unit of area, $Q(t)$, traversing the membrane to the thickness of the membrane l, to the concentration of diffusant at the upstream side of the membrane C_1 and to the diffusion coefficient D. In fact, only four terms of this summatory are

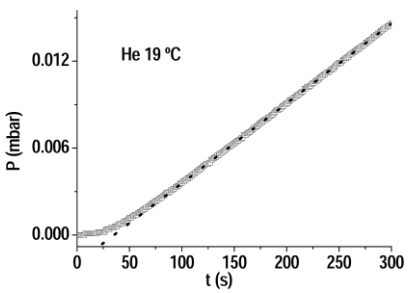

Fig. 2. Flow curve for He, showing the fitting of the steady state to a straight line.

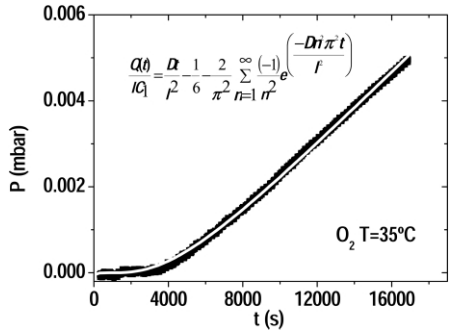

Fig. 3. Flow curve for oxygen showing the fitting of the whole curve with Eq. (2).

enough for correct fitting of our pressure vs time curves:

$$\frac{Q(t)}{lC_1} = \frac{Dt}{l^2} - \frac{1}{6} - \frac{2}{\pi^2}\sum_{n=1}^{\infty}\frac{(-1)}{n^2}\exp\left(\frac{-Dn^2\pi^2 t}{l^2}\right) \quad (2)$$

the diffusion coefficient is directly obtained from the fitting and the solubility coefficient is directly proportional to C_1. The permeability P is obtained as $SD = P$. Calculation of the uncertainties in the diffusion coefficients have been performed in the following way:

$$\sigma = 100\frac{[|\frac{L\epsilon(L)}{3\theta}|+|\frac{L^2\epsilon(\theta)}{6\theta^2}|]}{D} \quad (3)$$

where L is the thickness, θ is the time lag and D is the diffusion coefficient. Uncertainties, both in permeability and diffusivity, are about a 20%.

Examples of the flow curves thus obtained and the fits performed are shown in Figs. 2 and 3. An accurate determination of the leak rate of the apparatus is essential specially when low flow rates are being measured, as is the case of the experiments performed with oxygen in this work; Fig. 3 shows the corrected flow curve of one of the experiments perfomed with oxygen at 35 °C. Though the leak rate is of the same order as the flow caused by the diffusion of oxygen through the membrane, the corrected flow curves obtained can be easily fitted using Eq. (2).

3. Results and discussion

3.1. Temperature variation of the helium transport coefficients

The transport coefficients of helium have been measured in the temperature range of 5–40 °C and those of oxygen at 35 °C. The temperature range in which measurements have been made comprises the glass transition, which appears in the temperature range 5–30 °C by DSC (Fig. 1). Permeability, diffusivity and solubility appear collected in Table 1 and the temperature variation of P, D and S for helium are depicted in Figs. 4–6. As shown in Fig. 4, the temperature variation of permeability suffers a change in

Table 1
Helium transport coefficients at 1 bar

T (°C)	$D \times 10^7$ (cm^2 s^{-1})	$S \times 10^4$ (cm^3(STP)/cm^{3}cm Hg)	P (barrer)
5	4.3	1.31	0.56
10	5.4	1.31	0.72
16	6.2	1.53	0.95
19	7.5	1.55	1.16
22	7.7	1.61	1.24
25	8.0	1.67	1.33
28	10.7	1.71	1.84
31	12.6	1.7	2.14
34	13.9	1.8	2.45
37	15.8	1.8	2.86
40	17.2	1.9	3.34

slope at about 28 °C; Fig. 5 shows the solubility increase with temperature, though it is not possible to assess whether a change in slope at the T_g takes place because of the very small values of solubility. In Fig. 6, the diffusion coefficient variation with temperature appears depicted in Arrhenius coordinates. In the range of T_g, there seems to be a double break, a feature which is sometimes seen when studying diffusivity across the glass transition in some gas/polymer systems. Up to now, there is no general rule enabling to predict which pairs polymer/gas will show them. For example, helium shows double breaks at the glass transition in poly(vinyl acetate) (PVAC), single breaks in poly(ethylene terephthalate) (PET) and no breaks in poly(vinyl chloride) (PVC) or poly(ethyl methacrylate) (PEMA) [12]. Breaks at the glass transition are said to be due to differences in the diffusion activation energy below and above the glass transition [12,23], though it has to be taken into account that sometimes a double break at the glass transition takes place, and, however, no differences in the diffusion activation energies are seen. This is the case for He in poly(vinyl acetate), and in the PCR4MA studied in this work. In fact, the behaviour of helium in PCR4MA and in polyvinyl acetate is very similar: the diffusion of He in polyvinyl acetate shows a double break at the T_g, which is at about 25 °C; the activation energy above and below the glass transition is the same, i.e. 22.4 kJ mol^{-1}. PCR4MA shows a double break, and the activation energy under and over the glass transition is similar, 25 kJ mol^{-1} under T_g and

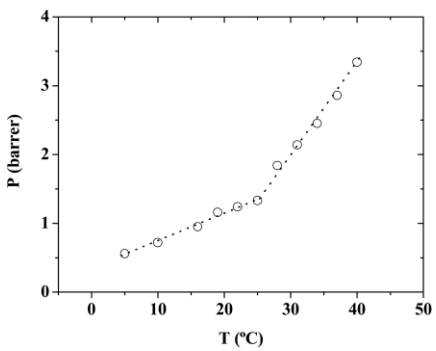

Fig. 4. Permeability of He as a function of temperature.

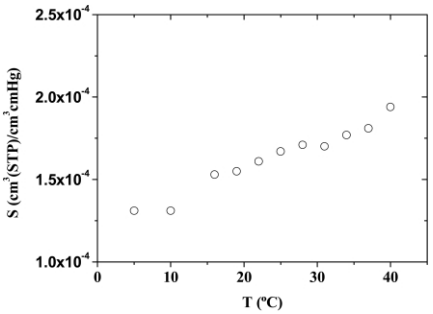

Fig. 5. Solubility of He as a function of temperature.

29.9 kJ mol^{-1} over T_g. Other authors [24] have proposed that the shape of the permeating gas and its size, related to the minimum critical volume in the polymer could be the cause of the changes in the activation energy at the glass transition.

Though, as pointed above, the temperature evolution of the helium diffusion coefficients is very similar in poly(vinyl acetate) (PVAC) and in PCR4MA, the actual diffusion coefficients are very different, even if the glass transition takes place almost at the same temperature. At 35 °C $D_{PVAC}(He) = 1.12 \times 10^{-5}$ cm^2 s^{-1} [26] and $D_{PCR4MA}(He) = 1.4 \times 10^{-6}$ cm^2 s^{-1}. At their respective T_g, $D_{PVAC}(He) = 8.1 \times 10^{-6}$ cm^2 s^{-1} ($T_g = 25$ °C) and $D_{PCR4MA} = 6 \times 10^{-7}$ cm^2 s^{-1} ($T_g = 15$ °C). In fact, the diffusion coefficients both for oxygen and helium are very small in this polymer, as is discussed in the next section.

3.2. Oxygen and helium transport coefficients at 35 °C

At 35 °C, i.e. just over the glass transition, the gas transport coefficients for helium and oxygen are those which appear in Table 2. As shown in the table the permeability of oxygen is extremely low, because both solubility and diffusivity are so. This table collects also gas transport coefficients of these two gases in another polymer, poly(2-[2-(2-ethoxyethoxy)ethoxy]ethyl methacrylate) PTEMA [17], a methacrylate with a linear side-chain consisting of three oxyethylene units, i.e. a polymer which contains the same ether units as PCR4MA, not as a cycle but as a linear

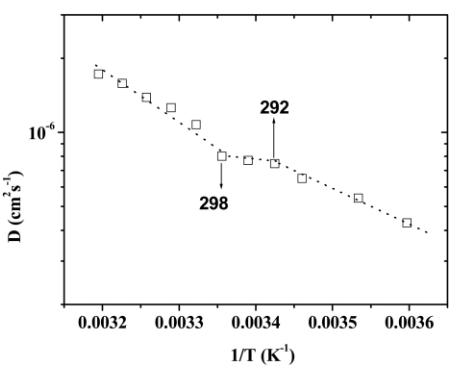

Fig. 6. Diffusivity of He as a function of temperature in Arrhenius coordinates.

Table 2
Transport data of helium and oxygen at 35 °C in the two methacrylic backbone polymers

Sample	Oxygen			Helium		
	P (barrer)	$D \times 10^8$ ($cm^2\ s^{-1}$)	$S \times 10^4$ (cm^3(STP) cm^{-3} cm Hg^{-1})	P (barrer)	$D \times 10^8$ ($cm^2\ s^{-1}$)	$S \times 10^4$ (cm^3(STP) cm^- cm Hg^{-1})
P4CRMA	0.006	0.5	1.3	2.45	140	1.8
PTEMA	3.9	140	2.8	14.4	1700	0.85

chain. The glass transition temperature and the FFV of this polymer appear collected in Table 3, together with other methacrylic polymers. The FFV has been obtained in all cases by applying Eq. (1), being the estimation of the occupied volume performed either by group contribution or by means of simulation programs like Hyperchem. The

Table 3
Oxygen transport data at 35 °C in various polymethacrylates

Sample	$D \times 10^8$ ($cm^2\ s^{-1}$)	$S \times 10^4$ (cm^3(STP) cm^{-3} cm Hg^{-1})	T_g (K)	FFV
PMMA [26]	0.39	2.5	379	0.121
P4CRMA	0.5	1.3	278	0.135
PtBMA [20]	10.8	4.2	392	0.188
PEMA[a] [16]	11.5	1.6	338	0.151
PEEMA [17]	20	7.3	257	0.201
PDEMA [17]	38	37	229	0.195
PTEMA [17]	140	2.8	218	0.191
CP3 [14]	175	41.3	≈220	0.191

PtBMA: poly(*t*-butyl methacrylate; PEEMA poly((2-ethoxyethoxy) ethoxy]ethyl methacrylate); PDEMA poly(2-(2-ethoxyethoxy)ethoxy]ethyl methacrylate); CP3 90/10 copolymer of dodecyl and ethyl methacrylate. The rest as defined in the text.

[a] At 25 °C.

Table 4
Diffusion of He and O_2 in some polymers at 25 °C

Polymer	T_g (K)	FFV	$D_{He} \times 10^8$ ($cm^2\ s^{-1}$)	$D_{Ox} \times 10^8$ ($cm^2\ s^{-1}$)	α_D (He/O_2)
PMMA [26]	379	0.121	400	0.39	1025
PVC [28]	358	0.120	280	0.4	233
P4CRMA	288	0.223	140	0.5	280
PET [28]	343	0.152	170	1.2	142
PFS-*t* But [29]	471	0.137	≈555	1.2	447
PTFE [26]	433	0.153	81.1	1.5	53
PC [25]	423	0.164	673	4.1	164
PVAC	298	0.138	955	5.6	170
Butylrubber [28]	203	0.119	593	8.1	73.2
6FDA-6FpDA [30]	593	0.272	740	9	82
PEMA [16]	338	0.151	4250	10.6	401
PS [26]	373	0.177	1040	11	94
Polychloroprene [26]	223	0.191	6040	101	60
PTEMA [28]	218	0.191	1700	140	12.1
Polybutadiene(*cis*) [26]	183	0.177	1550	150	10
Poly(isoprene) [28]	200	0.156	2160	173	12.5
PDMS [25]	150	0.33	10000	4100	2.4

Data for PTEMA, PDMS, 6FDA-6FpDA, PC, PTFE and P4CRMA are at 35 °C. PDMS poly(dimethyl siloxane); PS poly(styrene); PC Bisphenosl-A polycarbonate; PFS-*t* But polysulfone. The rest as defined in the text.

solubility coefficient both for He and O_2 are very similar in PTEMA and PCR4MA. The solubility of gases in polymer matrixes is the sum of two contributions, (i) the condensability of the gas, which depends on the critical temperature of the gas itself and on the availability of excess free volume, and (ii) the interaction of the gas with the polymer matrix. The chemical composition of both polymers is very similar, so no large differences in the interaction of helium and oxygen with the matrix are to be expected. On the other hand, helium and oxygen are not very condensable gases, so the contribution of gas condensability cannot differ much in PTEMA and PCR4MA. Thus, very similar solubility coefficients are to be expected (Scheme 2).

However, the diffusion coefficients are largely different in these two methacrylates: the diffusion coefficient of oxygen in PTEMA is 280 times greater than in PCR4MA, and 12 times in the case of helium. In fact, the diffusion coefficients in PCR4MA are among the lowest found in the literature, especially for He. This can be seen in Table 4, which collects data on He and O_2 diffusivity in polymers of very different structure, together with the glass transition temperatures and FFV of the polymers. As in the case of the polymers collected in Table 3, the FFV has been obtained in all cases by applying Eq. (1), being the estimation of the occupied volume performed either by group contribution or by means of simulation programs like Hyperchem. At 25 °C the diffusivity of He in this membrane is $8 \times 10^{-7}\ cm^2\ s^{-1}$. For example, at the same temperature the diffusion coefficient of He in butyl rubber [26] is $6 \times 10^{-6}\ cm^2\ s^{-1}$, for natural rubber [28] $22 \times 10^{-6}\ cm^2\ s^{-1}$, silicone rubber [24] $100 \times 10^{-6}\ cm^2\ s^{-1}$; even in glassy polymers, values of the diffusion coefficient are over 10 times the value obtained for this polymer. In polyvinyl acetate, which has roughly the same glass transition temperature, it is $9.8 \times 10^{-6}\ cm^2\ s^{-1}$ and in poly(ethylene terephthalate), which is a barrier polymer, i.e. a polymer with very low

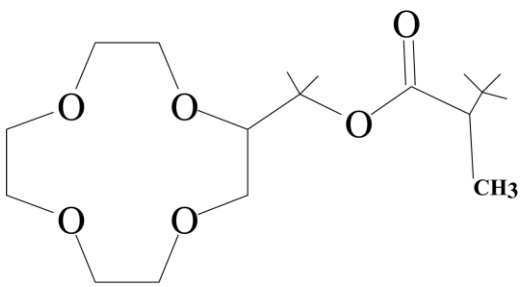

Scheme 2. Chemical structure of PCR4MA.

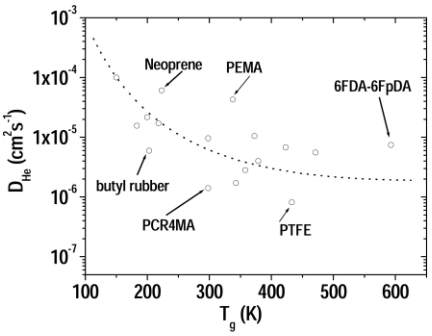

Fig. 7. Diffusivity of He in a set of polymers as a function of their glass transition.

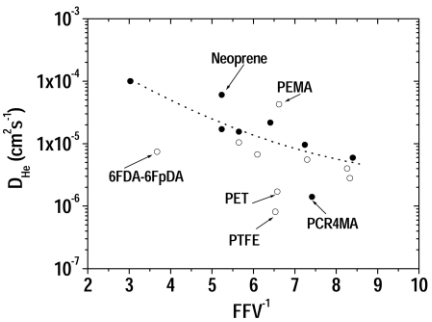

Fig. 8. Diffusivity of He in a set of polymers as a function of their FFV at 25 °C. Membranes measured under the glass transition are represented in open symbols, membranes measured over their glass transition are represented in solid symbols.

values of permeability, it is 1.7×10^{-6} cm^2 s^{-1}. As a result of the very low diffusivity and low solubility, the permeability of this material to He is among the smallest in the literature [25–27], and certainly much lower than values reported for materials with similar T_g.

Are these low diffusivity values to be expected? Figs. 7–12 show the dependence of the diffusion coefficients of He and O_2 on the two features which are frequently related to diffusivity, i.e. glass transition temperature and FFV. Figs. 7 and 10 show the dependence of the diffusion coefficients of helium and oxygen with the glass transition temperature. Obviously a rough correlation exists, and the

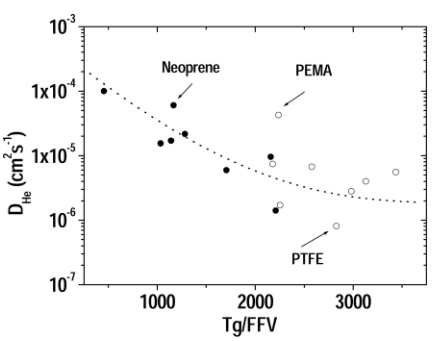

Fig. 9. Diffusivity of He in a set of polymers as a function of the ratio between their glass transition and FFV at 25 °C. Membranes measured under the glass transition are represented in open symbols, membranes measured over their glass transition are represented in solid symbols.

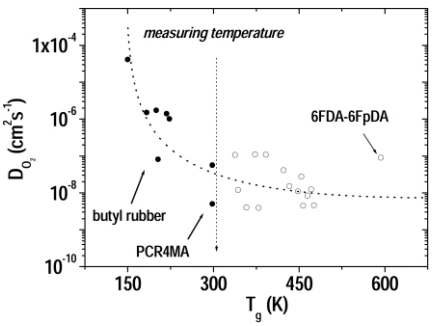

Fig. 10. Diffusivity of oxygen in a set of polymers as a function of their glass transition.

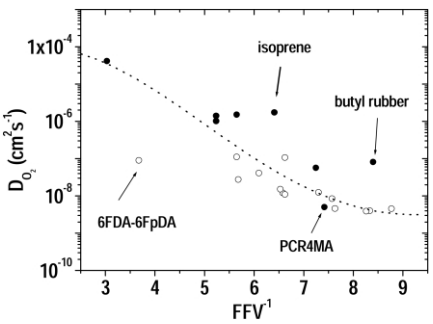

Fig. 11. Diffusivity of oxygen in a set of polymers as a function of their FFV at 25 °C. Membranes measured under the glass transition are represented in open symbols, membranes measured over their glass transition are represented in solid symbols.

lower the glass transition, the higher the diffusivity of gases; when the glass transition is well over the measuring temperature, the diffusivity ceases to depend on its proximity. For instance in the case of oxygen, the diffusion coefficients lie between 4×10^{-9} and 1×10^{-7} cm^2 s^{-1} for membranes with glass transitions between 338 and 690 K.

As mentioned above, the correlation between T_g and D is rather rough, however, some polymers deviate more clearly from it than others: He and O_2 diffusion coefficients in butyl rubber are much lower than expected according to its T_g, and the same happens with our PCR4MA and in

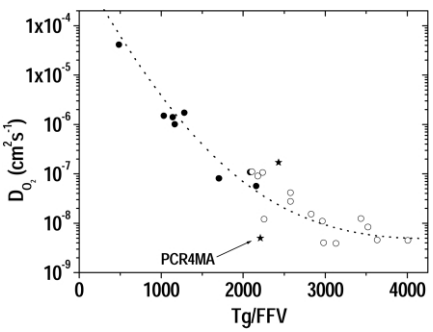

Fig. 12. Diffusivity of oxygen in a set of polymers as a function of the ration between their glass transition and FFV at 25 °C. Membranes measured under the glass transition are represented in open symbols, membranes measured over their glass transition are represented in solid symbols. PCR4MA and poly(dimethyl phenylene oxide) are represented by asterisk.

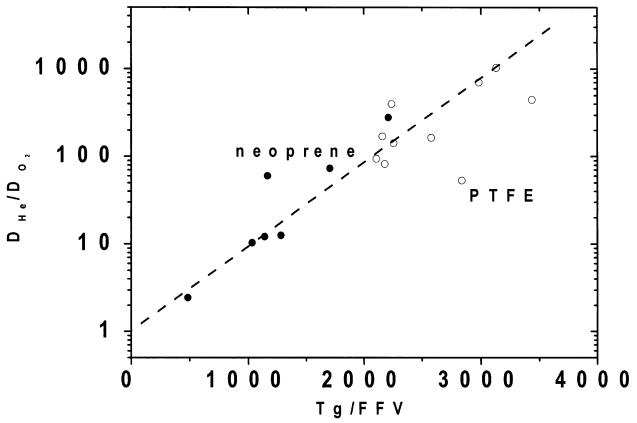

Fig. 13. Diffusivity selectivity for the gas pair O_2/He as a function of the ratio T_g/FFV. Membranes measured under the glass transition are represented in open symbols, membranes measured over their glass transition are represented in solid symbols.

poly(tetrafluoroethylene) (PTFE); on the opposite, He and O_2 diffusion coefficients are much higher than expected in polyethyl methacrylate and in hexafluoro dianhydride 4, 4′ hexafluoro diamine polyimide called 6FDA-6FpDA hereafter.

Figs. 8 and 11 show the, again rough correlation between the inverse of FFV and the diffusivity. In this case, for both studied gases, the diffusion coefficients are lower than would be expected for 6FDA-6FpDA and poly(tetrafluoroethylene), and higher for isoprene and butyl rubber in the case of oxygen, and poly(ethyl methacrylate) and polychlorprene in the case of He.

Our polymer, PCR4MA, does not deviate from the general trend which correlates FFV and the diffusion coefficient of oxygen (Fig. 11), and deviates somewhat in the case of He (Fig. 8); however, while the correlation between FFV and D_{oxygen} is quite good, this is not the case of the correlation between FFV and D_{helium}. Then, it can be assessed that the results obtained for this polymer are those expectable according to its FFV, and not so much according to its T_g.

In general, in membranes which have very large T_g, such as 6FDA-6FpDA, the diffusion coefficients are lower than expected when represented as a function of the FFV. In the same way, membranes which have very low FFV show D which are lower than expected when represented a function of T_g, this is the case for butyl rubber and our PCR4MA.

If both features, T_g and FFV, are taken together, as is done in Figs. 10 and 12, the correlation for oxygen is much improved, but not for He. In fact Fig. 12 shows that only PCR4MA and poly(dimethyl phenylene oxide) deviate rather strongly from the overall behaviour, the former negatively and the latter positively. Thus, though the transport data of this polymer are not anomalous, PCR4MA is in fact among the polymers which show the lower diffusion values both for He and O_2, taking into account its density, FFV and T_g.

Finally, the diffusivity selectivity $\alpha_D(He/O_2)$ as a function of the ratio T_g/FFV is shown in Fig. 13. A clear correlation between the diffusivity selectivity and the T_g/FFV ratio is seen, a single correlation which includes data obtained measuring below and above the glass transition. As expected the correlation extrapolates to 1 for very small values of the ratio T_g/FFV, i.e. either very low glass transitions or very high FFV or a combination of both. Again, some polymers deviate more strongly, namely poly(ethyl methacrylate), polychloroprene and PCR4MA positively and poly(tetrafluoroethylene) negatively. In the case of poly(ethyl methacrylate) and poly(chloroprene) the deviation is due to very high values of the diffusion coefficient of helium (Fig. 9), while in the case of poly(tetrafluoroethylene) to the opposite (Fig. 9); in the case of PCR4MA rather by very low values of the oxygen diffusion coefficient (Fig. 12). Mistaken estimation of the FFV could also bring about these deviations: it should be over-estimation of FFV in the case of poly(tetrafluoroethylene) and PCR4MA and underestimation for polychloroprene and poly(ethyl methacrylate); however, these polymers give no especially deviated results in Fig. 8, which represents the diffusion coefficients of oxygen as a function of the FFV.

Acknowledgements

We would like to acknowledge financial support from the Consejería de Cultura de la Comunidad de Madrid (BIO-009-2000).

References

[1] Pedersen CJ. The discovery of crown ethers. Nobel lecture 1987;8.
[2] Turro NJ, Kuo PL. J Phys Chem 1986;90:837–41.
[3] Habaue S, Morita M, Okamoto Y. Macromolecules 2002;35:2432–4.
[4] Feng X, Yan L, Wen J, Pan C. Polymer 2002;43:3131–7.
[5] Percec V, Randall R. Macromolecules 1989;22:4408–12.
[6] Roks MFM, Nolte RJM. Macromolecules 1992;25:5398–407.
[7] Privalko VP, Khaenko ES, Grekov AP, Savelyev Yu. Polymer 1994; 35:1730–8.
[8] Nishide H, Kawakami H, Suzuki T, Azechi Y, Soejima Y, Tauchida E. Macromolecules 1991;24:6306–9.
[9] Nishide H, Ohyanagi M, Okada O, Tsuchida E. Macromolecules 1986;495–6.
[10] Nishide H, Ohyanagi M, Okada O, Tsuchida E. Macromolecules 1987;417–22.
[11] Wang C, Chen C, Cheng HC, Chen CY, Kuo JF. J Membr Sci 2000; 177:189–99.
[12] Stern SA, Vakil UM, Mauze GR. J Polym Sci, Part B: Polym Phys 1989;27:405–29.
[13] Min KE, Paul DR. J Polym Sci, Part B: Polym Phys 1988;26: 1021–33.
[14] Tiemblo P, Fernández-Arizpe A, Riande E, Guzmán J. Polymer 2003; 44:635–41.

[15] Chiou JS, Paul DR. J Membr Sci 1989;45(1–2):167–89.
[16] Stannet V, Williams JL. J Polym Sci, Part C 1965;45–9.
[17] Tiemblo P, García F, García JM, García C, Riande E, Guzmán J. Polymer 2003; 44:2661–8.
[18] Mogri Z, Paul DR. Polymer 2001;42:7781–9.
[19] Mogri Z, Paul DR. Polymer 2001;42:2531–42.
[20] Wright CT, Paul DR. Polymer 1997;38:1871–8.
[21] Reinecke H, Finkelmann H. Makromol Chem 1992;193:2945–60.
[22] Hyperchem, Computational chemistry, version 5.01, Hypercube Inc., Ont., Canada; 1999.
[23] Crank J, Park GS, editors. Diffusion in polymers. London: Academic press; 1968. p. 58–9.
[24] Charati SG, Stern SA. Macromolecules 1998;31:5529–35.
[25] Handbook of gas diffusion in solids and melts. In: Shelby JE, editor. ASM International; 1996. Chapter 6.
[26] Thran A, Kroll G, Faupel F, Part B:. J Pol Sci: Polym Phys 1999;37: 3344–58.
[27] Pauly S. Permeability and diffusion data. In: Bandrup J, Immergut EH, Grulke AEJ, editors. Polymer handbook, 4th ed. Wiley, p. VI/543–69.
[28] Tiemblo P, Guzmán J, Riande E, Mijangos C, Reinecke H. Polymer 2001;4817–23. and corrigendum Polymer, 42; 2001, p. 8321.
[29] García C, Tiemblo P, Lozano AE, De Abajo J, de la Campa JG. J Membr Sci 2002;205:73–81.
[30] Costello LM, Koros WJ. J Pol Sci, Part B: Polym Phys 1995;33: 135–46.